Hydrogen Abstraction by Soybean Lipoxygenase-1. Density Functional Theory Study on Active Site Models in Terms of Gibbs Free Energies

Ismael Tejero,[†] Leif A. Eriksson,*[,‡] Àngels González-Lafont,[†] Jordi Marquet,[†] and José M. Lluch*[,†]

Departament de Química, Universitat Autònoma de Barcelona, 08193 Bellaterra, Barcelona, Spain, Department of Science, Örebro University, 701 82 Örebro, Sweden, and Department of Cell and Molecular Biology, Box 596, Uppsala University, 751 24 Uppsala, Sweden

Received: February 9, 2004; In Final Form: June 22, 2004

We herein report a density functional theory study of the rate-limiting hydrogen abstraction reaction from the C11 position of linoleic acid (here modeled by means of a (*Z*,*Z*)-2,5-heptadiene), by an Fe(III)−OH^- of soybean lipoxygenase-1 enzyme. Two active site models of the first coordination sphere of the active site were used. In the *small* model, we have represented histidines by ammonia, isoleucine by a formic anion, and asparagine by a formamide, whereas in the *large* model, we used imidazole rings to replace the histidines. No significant electronic differences between the two models were found. However, in the large model an important steric hindrance exists in the entrance channel of the substrate as it approaches the oxygen atom attached to the iron. A Gibbs free energy barrier as high as 20.8 kcal/mol at room temperature was in this case obtained for the hydrogen abstraction. However, the analysis of the factors which determine that value permits the prediction of a notoriously smaller barrier in the complete enzyme.

1. Introduction

Soybean lipoxygenase-1 (SLO-1) has received increasingly intense attention from both experimentalists and theoreticians for the past 10 years.[1−5] This is mainly due to the fact that the hydrogen atom abstraction catalyzed by SLO-1 exhibits the largest H/D kinetic isotope effect (KIE) on k_{cat} ($k_H/k_D = 81$ near room temperature) so far reported for a biological system.[6−9] This result provides compelling evidence for tunneling effects in an enzymatic reaction.

SLO-1 belongs to the family of lipoxygenases, a group of non-heme iron enzymes which use O_2 to stereo- and regiospecifically oxidize polyunsaturated fatty acids into fatty acid hydroperoxides.[10−13] In particular, SLO-1 catalyzes hydroperoxidation of 9(*Z*),12(*Z*)-octadecadienoic acid (linoleic acid) to 13(*S*)-hydroperoxy-9(*Z*),11(*E*)-octadecadienoic acid. At least 90% of the isolated SLO-1 is in its inactive high-spin ferrous form, which does not react with substrate and O_2. The catalytic iron center is in the high-spin ferric oxidation state in the active form of the enzyme. Magnetic circular dichroism studies of SLO-1 in solution show that its ferrous form is a mixture of five (5C)- and six (6C)-coordinate species (40% and 60%, respectively).[14] Addition of substrate shifts this equilibrium to a full conversion to the 6C species.[15] The 5C site includes three histidines (His499, His504, and His690), the monodentate carboxylate group of the C-terminal isoleucine (Ile839), and a water ligand. The sixth ligand, an asparagine (Asn694), has a very weak bonding interaction. No crystal data are available for the ferric form, although spectroscopic data seem to indicate that it is best described as 5C,[16] even in the presence of substrate, and that an OH^- ligand has replaced the water of the inactive form.

The generally accepted catalytic mechanism (see Scheme 1) proceeds by an initial, rate-limiting abstraction of the pro-*S* hydrogen atom from the C11 position of linoleic acid by an Fe(III)−OH^-, forming a substrate radical and Fe(II)−OH_2. O_2 rapidly reacts with the substrate radical, forming the hydroperoxide and regenerating the active form of the enzyme.

Recently, several theoretical studies have been devoted to the structure and catalytic reactivity of the active iron site of SLO-1. Borowski et al.[17] have performed density functional theory (DFT) calculations with the B3LYP functional and the LanL2DZ basis set for models of ferrous and ferric forms including the first coordination sphere. The corresponding amino acids were there substituted by their most relevant parts: histidines were replaced by imidazole rings, the C-terminal carboxyl group of isoleucine by a formic anion, and asparagine by a formamide molecule. Their results confirm the existence of both the 5C (although this structure is only found when the distance between Fe and oxygen of Asn694 is constrained at the experimental value, 3.05 Å) and the 6C species for the ferrous form. For the ferric form only the 6C species was found.

Lehnert et al.[18] employed the same level of calculations as Borowski et al.,[17] but replaced the histidines by ammonia, isoleucine by a formic anion, and asparagine by a formamide, using (*Z*,*Z*)-2,5-heptadiene as the substrate model. Their results show that Asn694 binds more weakly to Fe(III) than to Fe(II) due to the strong electron donor OH^- in the former, although in the absence of the second coordination sphere only a purely 6C structure is obtained in both cases. A one-dimensional potential energy surface, as a function of an approximately linear movement of the hydrogen atom from the carbon atom of the substrate to the hydroxyl ligand of Fe(III), exhibits a potential energy barrier for the hydrogen abstraction as high as 32 kcal/mol (34 kcal/mol after performing single-point energy calculations with the triple-ζ basis set TZV), which is reduced to about 27 kcal/mol when the zero-point energy correction is included

* Corresponding authors. E-mail: lluch@klingon.uab.es (J.M.L.).
[†] Universitat Autònoma de Barcelona.
[‡] Örebro University and Uppsala University.

10.1021/jp040114n CCC: $27.50
Published on Web 08/11/2004

SCHEME 1

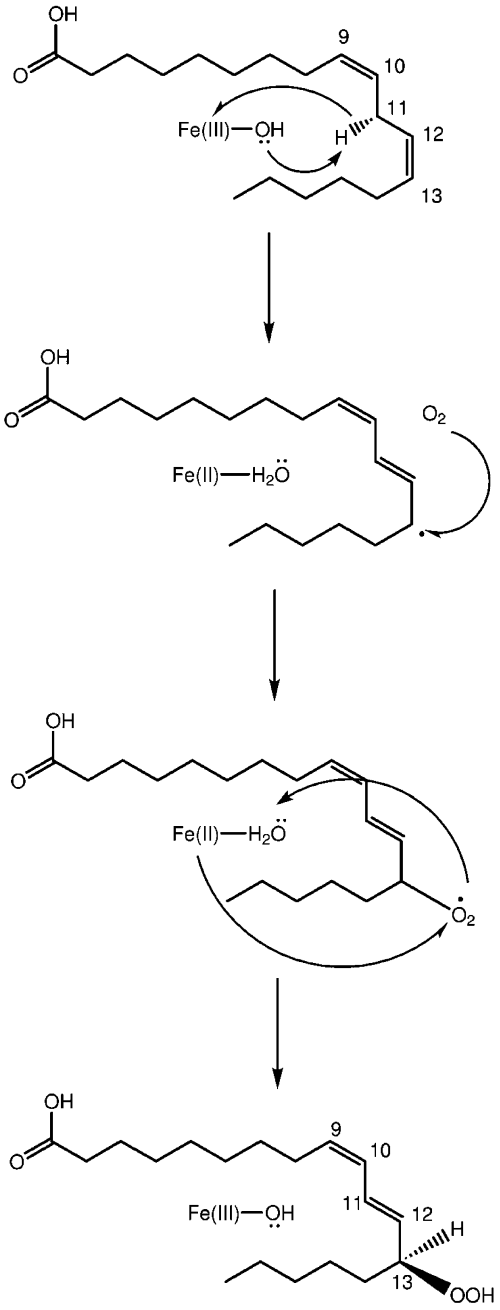

(the correction being assumed to be about 4−5 kcal/mol). This energy barrier was shown to be highly dependent on the hydrogen donor−hydrogen acceptor distance. Lehnert et al.[18] have estimated an energy barrier of about 15 kcal/mol (including the zero-point energy correction) at a C−O distance of around 2.7 Å.

Borowski and Broclawik[19] later used the same model as Lehnert et al.[18] to obtain a potential energy barrier for the hydrogen abstraction in the 6C ferric form of 12.1 kcal/mol at the B3LYP/6-311+G(d,p)//B3LYP/LanL2DZ level, including zero-point energy (ZPE) corrections calculated at the lower level. Finally, Tresadern et al.[20] have modeled the first coordination sphere of the 6C ferric form employing three imidazoles, one acetate, and one acetamide, along with OH^-, with 1,4-pentadiene as substrate. Using the PM3/d method with the appropriate iron parameters within their own semiempirical package, they obtained a potential energy barrier of 18.2 kcal/mol for the hydrogen abstraction.

From the above results it can be seen that a disparity of the energy barriers is observed for the hydrogen abstraction step, depending on the level of the electronic structure calculations. The explicit influence of the active site model used is not clear (for instance, the effect of using ammonia instead of imidazole ligands to represent histidines). In addition the entropic effects have not been considered. The purpose of this paper is to analyze theoretically, in terms of Gibbs free energies, the mechanism of the hydrogen abstraction reaction from the C11 position of linoleic acid (here modeled by means of a (*Z*,*Z*)-2,5-heptadiene) in a 6C ferric form of SLO-1, including the first coordination sphere. The results presented here will allow us to envisage some trends which are probably significant also when including a more complete model of the enzymatic system.

2. Computational Details

The unrestricted version of the three-parameter hybrid exchange-correlation functional B3LYP[21] has been tested in many previous computations of metalloenzymes,[22,23] and is known to give good agreement with experimental results. Looking at the size and the electronic complexity of the model used to study this hydrogen atom abstraction, density functional theory using the B3LYP functional seems to be the most suitable choice to carry out this work. All the calculations have been performed with the Gaussian 98 program package.[24]

Full geometry optimization and direct location of stationary points have been done with the Schlegel gradient optimization algorithm[25] employing the double-ξ basis set LanL2DZ[26,27] with an effective core potential (ECP) replacing the inner-shell electrons on the Fe atom. The characterization of both kinds of stationary points, minima or transition state structures, was carried out by diagonalizing their Hessian matrices and looking for zero or one negative eigenvalue, respectively. To ensure that each saddle point connects to their corresponding minima, intrinsic reaction coordinate (IRC)[28] calculations were performed. Thermodynamic and quasi-thermodynamic magnitudes were computed using the statistical thermodynamic formulation of partition functions within the ideal gas, rigid rotor, and harmonic oscillator models. Analytical second derivatives of the energy with respect to the Cartesian coordinates have been used for the determination of vibrational frequencies. The imaginary frequency is neglected in the ZPE and thermodynamic calculations of the transition-state structures. A standard state of 1 mol/L and a temperature of 298.15 K have been assumed in the calculations. From the optimized geometries, more accurate energies were obtained by performing B3LYP single-point energy calculations with a larger basis set, 6-311+G(d,p), including polarization and diffuse functions. A natural population analysis (NPA) according to the procedure developed by Weinhold and co-workers[29] was done to obtain the net charges and the spin distribution at the B3LYP/LanL2DZ electronic level.

3. Results and Discussion

Several groups have shown that the electronic effects on metalloenzyme catalyzed reaction mechanisms are very similar when using ammonia or imidazole as a model of histidine ligands.[30,31] However, as mentioned before, we are also interested here in the influence of the entropic effects, which could depend on the model size. Thus, for the sake of comparison, we initially used the same 6C ferric model as Lehnert et al.,[18] replacing histidines by ammonia, isoleucine by a formic anion, and asparagine by a formamide, and using (*Z*,*Z*)-2,5-heptadiene as a model of the substrate linoleic acid (LA).

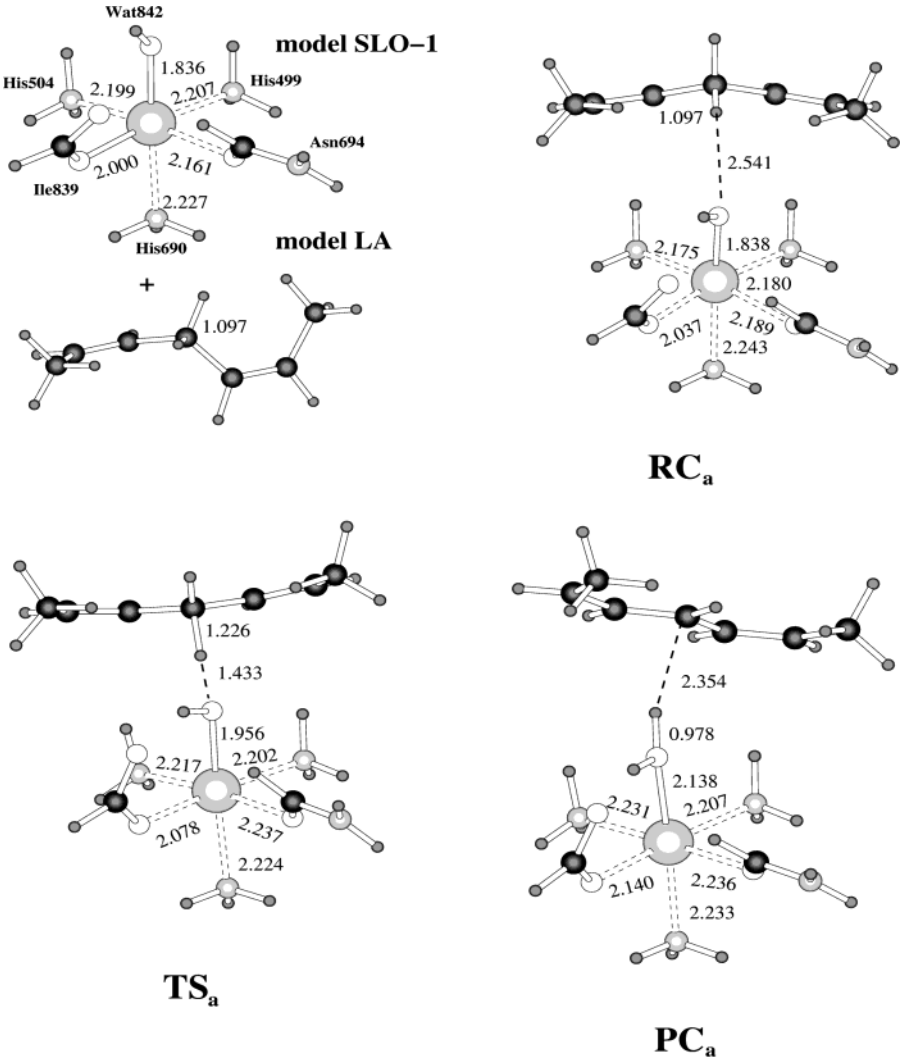

Figure 1. B3LYP/LanL2DZ stationary point structures related to the *small* model. Distances are given in angstroms.

TABLE 1: Classical Potential Energy (kcal/mol), Adiabatic Potential Energy (kcal/mol), Entropy (cal·K/mol), and Gibbs Free Energy (kcal/mol) for the B3LYP/LanL2DZ Stationary Points Found along the Reaction Path within the *Small* Model[a]

	B3LYP/LanL2DZ				B3LYP/6-311+G(d,p)//B3LYP/LanL2DZ			
	ΔV	$\Delta(V+\mathrm{ZPE})$	$\Delta S°$	$\Delta G°$	ΔV	$\Delta(V+\mathrm{ZPE})$	$\Delta S°$	$\Delta G°$
RC_a	−8.06	−7.07	−39.21	4.86	−6.03	−5.04	−39.21	6.89
TS_a	2.48	0.02	−38.24	11.55	8.94	6.47	−38.24	18.01
PC_a	−25.37	−26.34	−32.75	−15.9	−18.94	−19.91	−32.75	−9.47

[a] All magnitudes are relative to reactants at infinite distance.

In a second stage, we replaced the ammonia molecules in the first (*small*) model by imidazole rings and studied the hydrogen abstraction mechanism with this more complex system (*large* model).

3.1. Small Model. The structures of the B3LYP/LanL2DZ stationary points located for the hydrogen abstraction reaction are depicted in Figure 1. The corresponding energies and entropic contributions are collected in Table 1. Although one could imagine different conformations for the substrate in the active site model, only the reactant complex RC_a shown in Figure 1 was located as a minimum energy structure. It has a rather linear conformation which is very similar to the one found by Borowski and Broclawik.[19] The distance between the hydrogen atom which will be transferred (H_T) and the carbon atom to which it is attached (C_{LA}) remains the same as in the model of the isolated linoleic fragment, even though the substrate has adopted a different conformation in the RC_a structure. Due to the complex formation some Fe−ligand distances lengthen (Asn694, His690, and Ile839) or shorten (His504 and His499) slightly, while the Fe−O(Wat842) distance remains essentially unaltered. The computed classical potential energy of complexation is 8.1 kcal/mol, to which the formation of a weak hydrogen bonding interaction between H_T and O(Wat842) with a C_{LA}−O(Wat842) distance of 3.502 Å is the main contribution. In terms of adiabatic energy, that is, the classical potential energy + ZPE correction, the stability of the reactant complex is reduced by 1 kcal/mol. Entropic effects clearly disfavor the formation of RC_a, in that it lies 4.86 kcal/mol above the reactants in terms of the Gibbs free energy.

The imaginary frequency of the transition state structure (TS_a) has a value of 952i cm^{-1}. IRC calculations were performed to verify that it connects RC_a with the product complex PC_a. Going from RC_a to TS_a, five of the Fe−ligand distances increase slightly, with the most significant change being the Fe−

O(Wat842) distance (from 1.838 to 1.956 Å). Only the Fe−His690 distance displays a slight decrease. The $C_{LA}-H_T$ distance increases from 1.097 to 1.226 Å while the O(Wat842)$-H_T$ distance decreases from 2.541 to 1.433 Å. The $C_{LA}-$O(Wat842) distance becomes 2.659 Å in TS_a, indicating a clear approach between the substrate and the active site model of SLO-1. As can be seen in Table 1, the classical potential energy barrier with respect to RC_a is 10.5 kcal/mol. This value is significantly lower than the barrier given by Lehnert et al. (32 kcal/mol),[18] obtained using the C−O distance frozen to the value corresponding to the crystallographic data (about 3 Å).[1] However, Lehnert et al. also noted that the potential energy barrier was greatly reduced when the substrate was brought closer to the active site. In our calculations the $C_{LA}-$O(Wat842) distance is reduced about 0.84 Å from RC_a to TS_a, which allows for the significant reduction of the energy barrier. When ZPE corrections are included, our adiabatic potential energy barrier goes down to 7.1 kcal/mol. No significant entropic differences between RC_a and TS_a exist, with the free energy barrier being slightly more reduced, to 6.7 kcal/mol.

The final stationary point shown in Figure 1 is the product complex PC_a, in which the orientation with respect to the active site model is somewhat different. Again the most significant variation in the Fe−ligand distances corresponds to the Fe−O(Wat842) bond, which increases from 1.956 (TS_a) to 2.138 Å (PC_a). The water molecule (Wat842) thereby formed has an O(Wat842)$-H_T$ distance of 0.978 Å. The exoergicity of the formation of PC_a with respect to RC_a turns out to be 17.3 (19.3) kcal/mol without (with) inclusion of ZPE effects. The formation of PC_a from TS_a is entropically favored, in such a way that the exergonicity from RC_a is 20.8 kcal/mol.

The B3LYP/6-311+G(d,p)//B3LYP/LanL2DZ calculations allows for a comparison with the results of Borowski and Broclawik.[19] The potential energies, entropies, and free energies were obtained using the B3LYP/LanL2DZ geometries and frequencies (see Table 1). The classical potential energy barrier, the adiabatic energy barrier, and the free energy barrier are 15, 11.5, and 11.1 kcal/mol, respectively, with respect to RC_a. The adiabatic barrier is slightly smaller than the value of 12.1 kcal/mol calculated by Borowski and Broclawik. The discrepancy of 0.6 kcal/mol could be attributed either to a difference between the two reactant complexes (no information about the reactant complex is provided in that paper) or to a variation in the orientation of the formamide representing Asn694 in the two transition state structures (at the transition state structure in the paper by Borowski and Broclawik the formamide seems to be 180° twisted around the C−O bond with respect to the transition state structure located in the present work).

3.2. Large Model. The structures of the stationary points located at the B3LYP/LanL2DZ level are depicted in Figure 2. The corresponding energetic and entropic magnitudes are collected in Table 2. Without geometric restrictions, the optimization on the second model system leads to a reactant complex RC_i which is stabilized by 5.1 (4.5) kcal/mol without (with) inclusion of ZPE effects, with respect to the isolated reactants. As can be seen, the values are smaller than the ones corresponding to the reactant complex RC_a. Due to the unfavorable entropic effects, the free energy of RC_i lies 4.85 kcal/mol higher than the isolated reactants. The similar value of $\Delta G°$ for the small and the large models is a result of the compensation between a more negative classical potential energy for the formation of RC_a in the ammonia model and a smaller loss of entropy in the large imidazole ring model. As seen in Figure 2, the substrate fragment of RC_i is oriented very differently compared to that obtained for RC_a. H_T is too far from O(Wat842) (5.921 Å) to form a $C_{LA}-H_T\cdots$O(Wat842) hydrogen bond. Instead, the complexation energy is due to the existence of an N−H···C hydrogen bond interaction between His499 and (*Z*,*Z*)-2,5-heptadiene. Due to the early character of RC_i along the reaction path, no significant change of the Fe−ligand distances is observed during the formation of the reactant complex.

The imaginary frequency of the transition state structure (TS_i) has a value of 1094.7i cm^{-1}. IRC calculations from TS_i clearly showed that this connects RC_i with the product complex PC_i. The relative position of the substrate fragment in TS_i is somewhat different from the ones in TS_a, although the difference is much reduced compared to that seen for RC_i and RC_a (compare Figures 1 and 2). The values of the $C_{LA}-H_T$ and O(Wat842)$-H_T$ distances, 1.245 and 1.409 Å, respectively, show that TS_i is a later transition state than TS_a. The $C_{LA}-$O(Wat852) distance in TS_i is 2.654 Å, essentially the same value as in TS_a. As seen upon a comparison between Figures 1 and 2, the local geometry of the substrate is very different in the large model. In the small model the lipid is "W"-shaped, whereas in the large model, the substrate is "S"-shaped, despite the starting point for the optimizations being the "W"-shaped form.

The structural differences between the reactant complexes and the transition state structures of both models provoke, as seen comparing Tables 1 and 2, striking changes in the values of energy and entropy. Thus, the classical potential energy barrier and the adiabatic potential energy barrier with respect to RC_i turn out to be 15.8 and 12.7 kcal/mol, respectively, more than 5 kcal/mol larger than the corresponding values for the small model. In turn, conversely to the case of small model, the entropy barrier is now negative, such that the free energy barrier becomes 15.4 kcal/mol, more than twice that when using ammonia. These differences can be easily understood by comparing the structures depicted in Figures 1 and 2. The substrate has to approach the oxygen atom which will evolve to Wat842, to enable a hydrogen transfer with a low potential energy barrier. The access to O(Wat842) is relatively free in the small model, whereas in the large model with imidazoles representing His499 and His504 these clearly hinder the approach of a sizable substrate as (*Z*,*Z*)-2,5-heptadiene (albeit this still being a short model of the actual substrate, linoleic acid). As a consequence, the O(Wat842)$-H_T$ distance in RC_a is only 2.541 Å, whereas in RC_i the corresponding distance is as large as 5.921 Å. RC_i thereby becomes less stabilized than RC_a. When the substrate is forced to advance along the reaction path to reach the transition state structure, the steric hindrance in the entrance channel due to the imidazole rings becomes increasingly significant, in such a way that the potential energy of the reaction path of the large model is raised relative to the reaction path of the smaller model. This in turn leads to a considerable difference in the potential energy barriers of the two models. In addition, the entropic term is clearly unfavorable for the approach of the substrate from a distant position with respect to O(Wat842) in RC_i to a close position in TS_i, in contrast to the insignificant role of the entropic term for the analogous, but much shorter, path from RC_a to TS_a.

In the product complex PC_i, Wat842 has been completely formed. All Fe−ligand distances except that corresponding to His690 slightly increase from the TS_i structure. The exoergicity of the formation of PC_i with respect to RC_i turns out to be 11.1 or 11.8 kcal/mol in terms of potential energy without or with

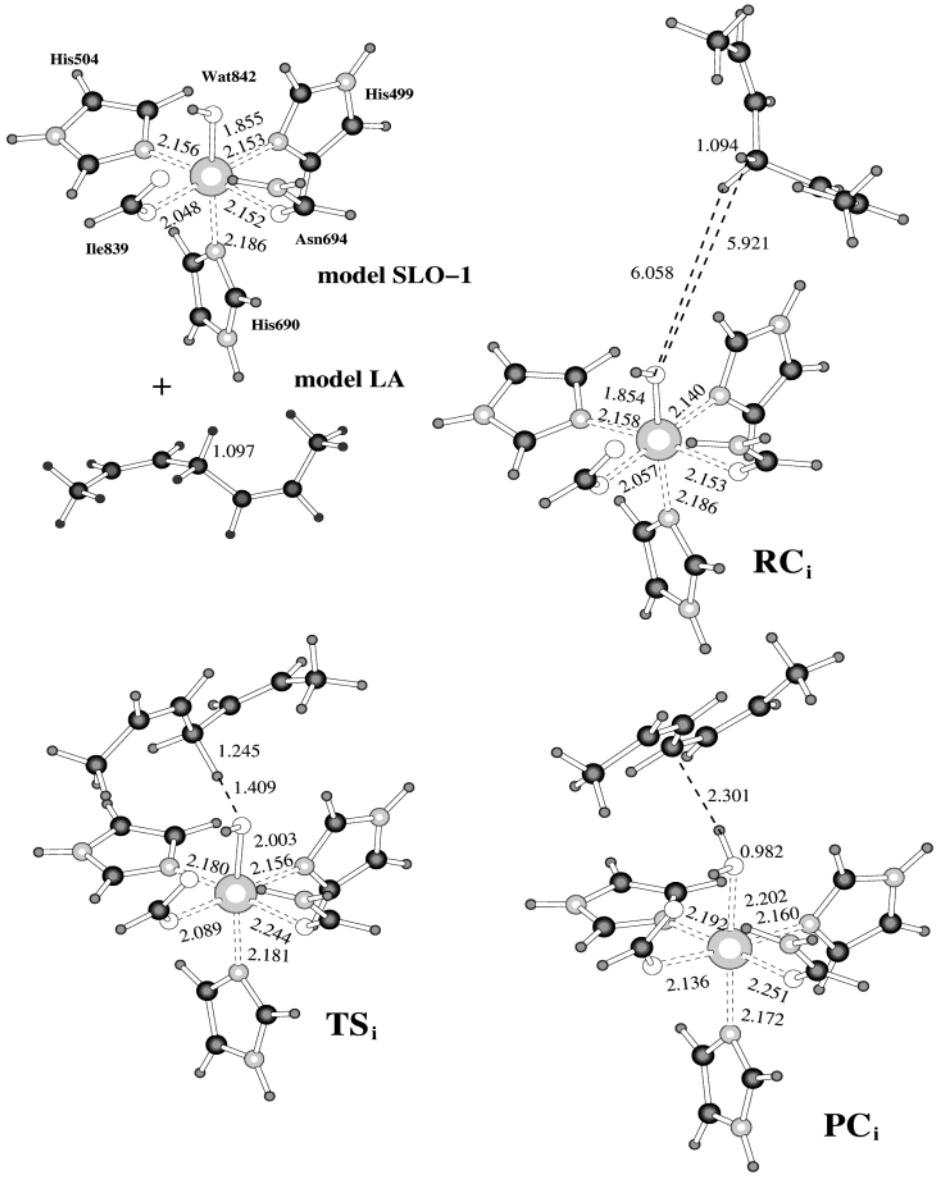

Figure 2. B3LYP/LanL2DZ stationary point structures related to the *large* model. Distances are given in angstroms.

TABLE 2: Classical Potential Energy (kcal/mol), Adiabatic Potential Energy (kcal/mol), Entropy (cal·K/mol), and Gibbs Free Energy (kcal/mol) for the B3LYP/LanL2DZ Stationary Points Found along the Reaction Path within the *Large* Model[a]

	B3LYP/LanL2DZ				B3LYP/6-311+G(d,p)//B3LYP/LanL2DZ			
	ΔV	$\Delta(V+\mathrm{ZPE})$	$\Delta S°$	$\Delta G°$	ΔV	$\Delta(V+\mathrm{ZPE})$	$\Delta S°$	$\Delta G°$
RC_i	−5.10	−4.52	−29.06	4.85	−4.36	−3.78	−29.06	5.59
TS_i	10.66	8.22	−39.55	20.26	16.75	14.31	−39.55	26.35
PC_i	−16.22	−16.36	−28.87	−6.67	−10.38	−10.52	−28.87	−0.83

[a] All magnitudes are relative to reactants at infinite distance.

ZPE correction, respectively. The free energy of the reaction is 11.5 kcal/mol at the B3LYP/LanL2DZ level.

At the B3LYP/6-311+G(d,p)//B3LYP/LanL2DZ electronic level the classical potential energy barrier, the adiabatic potential energy barrier, and the free energy barrier with respect to RC_i are 21.1, 18.1, and 20.8 kcal/mol, respectively. Comparing with the corresponding values for the small model, the B3LYP/6-311+G(d,p)//B3LYP/LanL2DZ results follow the same trends as the B3LYP/LanL2DZ results. The formation of PC_i with respect to RC_i is 6.0 kcal/mol (6.7 kcal/mol) exoergic without (with) inclusion of ZPE effects, and 6.4 kcal/mol exergonic.

3.3. Natural Population Analysis. We performed natural population analyses (NPA) of all the ligands and critical atoms in the stationary points located for both models. The results are shown in Tables 3 and 4. The evolution of the net charges and the spin distribution are quite analogous for the two models, thus confirming that ammonia and imidazole ligands exert similar electronic effects in these metalloenzyme catalyzed reaction mechanisms. In the following, we will thus primarily discuss the results corresponding to the large model. Along the reaction path, the main changes concern the critical atoms Fe, C_{LA}, and H_T, and the OH group of Wat842. Formally, the iron atom should be in its high-spin d^5 sextet ferric oxidation state (with a net charge of +3 and five unpaired electrons) in the reactant complex RC_i, and should evolve to the high-spin d^6 quintet ferrous oxidation state (with a net charge of +2 and

TABLE 3: Natural Population Analysis (au) in the Stationary Points Located for the *Small* Model along the Reaction Path

	reactants	RC_a	TS_a	PC_a
	Net Charge			
Fe	1.724	1.719	1.614	1.487
C_{LA}	−0.469	−0.502	−0.471	−0.243
H_T	0.219	0.242	0.336	0.523
OH(Wat842)	−0.483	−0.470	−0.492	−0.554
Asn694	0.096	0.089	0.067	0.053
Ile839	−0.714	−0.732	−0.764	−0.775
His504	0.139	0.136	0.101	0.084
His690	0.112	0.106	0.093	0.079
His499	0.125	0.124	0.103	0.085
	Spin Distribution			
Fe	3.996	3.992	3.869	3.721
C_{LA}	0.000	0.001	0.186	0.475
H_T	0.000	0.000	−0.005	0.002
OH(Wat842)	0.448	0.472	0.389	0.043
Asn694	0.084	0.075	0.049	0.035
Ile839	0.200	0.175	0.112	0.057
His504	0.108	0.116	0.071	0.051
His690	0.074	0.071	0.055	0.044
His499	0.089	0.097	0.068	0.051

TABLE 4: Natural Population Analysis (au) in the Stationary Points Located for the *Large* Model along the Reaction Path

	reactants	RC_i	TS_i	PC_i
	Net Charge			
Fe	1.765	1.783	1.515	1.529
C_{LA}	−0.469	−0.471	−0.432	−0.261
H_T	0.219	0.209	0.368	0.521
OH(Wat842)	−0.478	−0.493	−0.482	−0.533
Asn694	0.103	0.058	0.016	0.022
Ile839	−0.739	−0.723	−0.801	−0.771
His504	0.125	0.131	0.076	0.065
His690	0.098	0.108	0.078	0.075
His499	0.125	0.115	0.062	0.083
	Spin Distribution			
Fe	4.000	4.017	3.696	3.717
C_{LA}	0.000	0.000	0.271	0.466
H_T	0.000	0.000	0.014	0.002
OH(Wat842)	0.476	0.443	0.367	0.043
Asn694	0.075	0.087	0.036	0.030
Ile839	0.160	0.149	0.055	0.057
His504	0.113	0.111	0.060	0.046
His690	0.070	0.079	0.057	0.052
His499	0.103	0.112	0.045	0.059

four unpaired electrons) in the product complex PC_i. From the population analyses, we find that the net charge and spin distribution varies from 1.783 to 1.529, and from 4.017 to 3.717, respectively, going from RC_i to PC_i. It is clear that the iron atom behaves neither as a formally pure Fe(III) nor as a pure Fe(II), although the change in electronic population agrees with the direction of that formally expected. The remaining groups of the active site model help in delocalizing both the net charges and the spin distribution. Thus, as expected, the total net charge of the iron atom and its 6C first coordination sphere is +1 in both RC_i and PC_i, whereas the total spin distribution is 5 in RC_i but 4 in PC_i. As the hydrogen abstraction proceeds, C_{LA} acquires a radical character (shared with the remaining atoms of the substrate), H_T increases its positive net charge while keeping a negligible spin distribution, and Wat842 becomes a neutral closed-shell water molecule. Then, in good agreement with the work by Lehnert et al.,[18] our results indicate that the mechanism of this hydrogen abstraction reaction can be described as a one-step process consisting of a concerted proton and electron transfer from the substrate to the iron atom and its first coordination sphere in the catalytic center of the enzyme. The proton becomes attached to the OH group of Wat842, whereas the electron is mainly distributed between the iron atom and the OH group.

4. Final Remarks

In this paper we have used two active site models to theoretically study the rate-limiting hydrogen abstraction reaction from the C11 position of linoleic acid (here modeled by means of a (*Z*,*Z*)-2,5-heptadiene) by an Fe(III)−OH^- of SLO-1 enzyme (here including the first coordination sphere of a 6C ferric form of SLO-1). In the small model, we have represented histidines by ammonia, isoleucine by a formic anion, and asparagine by a formamide, whereas in the large model we have used imidazole rings to replace the histidines.

Natural population analyses along the reaction path shows that the mechanism of this hydrogen abstraction reaction can be described as a one-step process consisting of a concerted proton and electron transfer from the substrate to the iron atom and its first coordination sphere. We have found no significant electronic differences between the two models, thus confirming that—in this respect—ammonia can be used instead of imidazole rings to represent histidines. However, the kinetics of the reaction highly depends on the model used. At the B3LYP/6-311+G(d,p)//B3LYP/LanL2DZ electronic level, the classical potential energy barrier, the adiabatic potential energy barrier, and the Gibbs free energy barrier for the larger model are 21.1, 18.1, and 20.8 kcal/mol, respectively, with respect to the reactant complex. The corresponding values for the small model turn out to be noticeably lower: 15, 11.5, and 11.1 kcal/mol, respectively. The most important difference concerns the Gibbs free energy. This discrepancy can be understood on the basis of the steric hindrance in the entrance channel of the substrate approaching the oxygen atom attached to the iron atom, due to the two imidazole rings. If ammonia is instead used to represent the histidines, the access to the oxygen atom is quite free. This result is important because it points out that not only electronic, but also steric effects have to be considered when a reliable, simplified reaction model is designed. In addition, the influence on not only the potential energy but also the Gibbs free energy has to be taken into account.

A final point concerns the relevance of the present results in order to understand the mechanism of the hydrogen abstraction reaction in the complete enzyme. A definitive response to this problem would require nuclear dynamics calculations on a reliable quantum mechanical/molecular mechanical[32−35] potential energy surface involving the whole enzyme and the actual substrate. This is particularly difficult for this iron-containing enzyme, because the right description of the transition metal requires at least a DFT calculation for the quantum mechanical region.[36] In the meantime, active site model calculations are useful because they provide valuable, preliminary information, although the results need to be taken with caution. In the present case, it is likely that the electronic description of the reaction in the active site model holds also in the whole enzyme. However, we think that this could not be true for the free energy barriers. We have seen above that with imidazole rings (but not using ammonia) the free energy barrier is as high as 20.8 kcal/mol with respect to the reactant complex. In this last structure the substrate is very far from the iron center when the active site model is considered, but it could be expected that the enzyme forces the substrate to approach the iron center, so destabilizing the reactant complex and diminishing the free energy barrier (due to both the energetic and the entropic contributions). In other words, as is well-known, the structure

TABLE 5: Classical Potential Energy Barriers (kcal/mol) within the *Large* Model for the Optimized Reactant Complex RC_i Keeping Frozen the $C_{LA}-O(Wat842)$ Distance (Å) at Different Values (See Text)

$C_{LA}-O(Wat842)$	B3LYP/ LanL2DZ	B3LYP/ 6-311+G(d,p)//B3LYP/LanL2DZ
6.45	15.76	21.11
4.00	13.66	18.87
3.50	13.16	18.08

of the SLO-1 enzyme is more optimal to receive the substrate as it is at the transition state structure than as it is at the reactant complex. Very recently, Hammes-Schiffer[37] and co-workers have studied the proton-coupled electron-transfer reaction catalyzed by SLO-1 with a multistate continuum theory that represents the transferring hydrogen nucleus as a quantum mechanical wave function. Interestingly, they obtained from docking calculations in linoleic acid and SLO-1 that a suitable conformation of the substrate involves a $C_{LA}-O(Wat842)$ distance of 2.83 Å. This distance is somewhat longer than that corresponding to our transition state structure TS_i (2.654 Å), but it shows that the reactant complex RC_i (that distance is 6.45 Å) is unable to be inserted in the active site of the real enzyme. Then, the reactant complex has to be largely destabilized to be accommodated inside the enzyme. To evaluate this energetic effect, we have reoptimized the reactant complex RC_i, keeping frozen the $C_{LA}-O(Wat842)$ distance in the shorter values of 4 and 3.5 Å. The respective classical potential energies relative to reactants at infinite distance turn out to be −3 and −2.50 kcal/mol at the B3LYP/LanL2DZ electronic level (compare with −5.10 kcal/mol for RC_i). At the higher B3LYP/6-311+G(d,p)// B3LYP/LanL2DZ electronic level the corresponding values are −2.12 and −1.33 kcal/mol, respectively (compare with −4.36 kcal/mol for RC_i). Then it is clear that compression of the reactant complex reduces the energy barrier. The classical potential energy barriers calculated with respect to the reactant complex RC_i for several $C_{LA}-O(Wat842)$ frozen distances are collected in Table 5.

On the other hand, in the absence of the second coordination sphere, only the six (6C)-coordinate structure for the ferric form exists. Therefore, the calculations presented in this paper have been done on such a 6C structure only. As mentioned in the Introduction, spectroscopic data[16] seem to indicate that the ferric form is best described as a five (5C)-coordinate site with one very long bond to Asn694. This 5C structure would destabilize the ferric state, thus reducing the free energy barrier. In the active site model just including the first coordination sphere, the 5C structure only can be obtained if the Fe−O(Asn694) distance is kept at the experimental value (2.87−3.05 Å). Constraining this distance at the value of 2.9 Å, and optimizing the remaining geometric parameters with the large model, we located the reactant complex $RC_i(5C)$ (see Figure 3). The structure of the five-coordinated reactant complex is comparable to the six-coordinated RC_i. Maintaining the Asn694 (represented by a formamide) weakly bonded to the iron center, we perceive a logical slight decrease of most of the other Fe−ligand distances. $RC_i(5C)$ turns out to be destabilized with respect to RC_i by 6.2, 6.1, and 6.3 kcal/mol in terms of classical potential energy, adiabatic energy, and Gibbs free energy, respectively. Since the transition state structure probably will have a structure intermediate between 5C and 6C first coordination sphere, a reduction of the free energy barrier of less than 6.3 kcal/mol would be expected. In all, from the results presented in this paper, a Gibbs free energy barrier notoriously smaller than 20 kcal/mol could be predicted for the hydrogen abstraction reaction from linoleic acid catalyzed by the soybean lipoxygenase-1 enzyme. This conclusion agrees with the results obtained by Olsson et al.[38,39] in two papers that appeared during the writing process of this work. Combining a quantum classical path (QCP) version of the centroid path integral approach with a DFT-based empirical valence bond (EVB) potential energy surface, Olsson et al. have found a quantum free energy barrier of 13.8 kcal/mol at 300 K for the hydrogen transfer from 1,4-pentadiene as substrate, adding the effect of the protein.

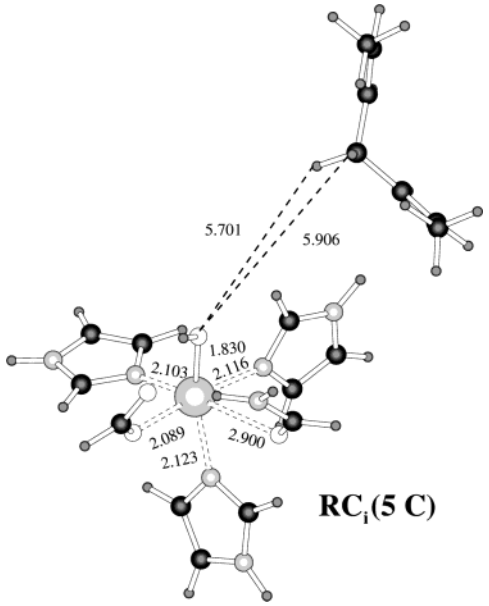

Figure 3. B3LYP/LanL2DZ structure corresponding to the complex RC_i (5C). Distances are given in angstroms.

Acknowledgment. We are grateful for financial support from the Spanish "Ministerio de Ciencia y Tecnología" through Project Nos. BQU2002-00301 and BQU2003-05457, and the Swedish Science Research Council (VR). The supercomputing center in Linköping (NSC) is gratefully acknowledged for computing time.

References and Notes

(1) Minor, W.; Steczko, J.; Stec, B.; Otwinowski, Z.; Bolin, J. T.; Walter, R.; Axelrod, B. *Biochemistry* **1996**, *35*, 10687.
(2) Tomchick, D. R.; Phan, P.; Cymborowski, M.; Minor, W.; Holman, T. R. *Biochemistry* **2001**, *40*, 7509.
(3) Rickert, K. W.; Klinmann, J. P. *Biochemistry* **1999**, *38*, 12218.
(4) Moiseyev, N.; Rucker, J.; Glickman, M. H. *J. Am. Chem. Soc.* **1997**, *119*, 3853.
(5) Knapp, M. J.; Rickert, K. W.; Klinmann, J. P. *J. Am. Chem. Soc.* **2002**, *124*, 3865.
(6) Glickman, M. H.; Wiseman, J. S.; Klinman, J. P. *J. Am. Chem. Soc.* **1994**, *116*, 793.
(7) Glickman, M. H.; Klinman, J. P. *Biochemistry* **1995**, *34*, 14077.
(8) Kohen, A.; Klinman, J. P. *Acc. Chem. Res.* **1998**, *31*, 397.
(9) Knapp, M. J.; Klinmann, J. P. *Eur. J. Biochem.* **2002**, *269*, 3113.
(10) Siedow, J. N. *Annu. Rev. Plant Physiol. Plant Mol. Biol.* **1991**, *42*, 145.
(11) Ford-Hutchinson, A. W.; Gresser, M.; Young, R. N. *Annu. Rev. Biochem.* **1994**, *63*, 383.
(12) Kühn, H.; Borngräber, S. In *Lipoxygenases and their metabolites*; Nigam, S., Pace-Asciak, C. R., Eds.; Plenum: New York, 1999; pp 5−28.
(13) Brash, A. R. *J. Biol. Chem.* **1999**, *274*, 23679.
(14) Pavlosky, M. A.; Solomon, E. I. *J. Am. Chem. Soc.* **1994**, *116*, 11610.
(15) Pavlosky, M. A.; Zhang, Y.; Westre, T. E.; Gan, Q. F.; Pavel, E. G.; Campochiaro, C.; Hedman, B.; Hodgson, K. O.; Solomon, E. I. *J. Am. Chem. Soc.* **1995**, *117*, 4316.
(16) Solomon, E. I.; Zhou, J.; Neese, F.; Pavel, E. G. *Chem. Biol.* **1997**, *4*, 795.
(17) Borowski, T.; Król, M.; Chruszcz, M.; Broclawik, E. *J. Phys. Chem. B* **2001**, *105*, 12212.
(18) Lehnert, N.; Solomon, E. I. *J. Biol. Inorg. Chem.* **2003**, *8*, 294.

(19) Borowski, T.; Broclawik, E. *J. Phys. Chem. B* **2003**, *107*, 4639.
(20) Tresadern, G.; McNamara, J. P.; Mohr, M.; Wang, H.; Burton, N. A.; Hillier, I. H. *Chem. Phys. Lett.* **2002**, *358*, 489.
(21) Becke, A. D. *J. Chem. Phys.* **1993**, *98*, 5648.
(22) Blomberg, M. R. A.; Siegbahn, P. E. M. *J. Phys. Chem. B* **2001**, *105*, 9375.
(23) Siegbahn, P. E. M.; Blomberg, M. R. A. *Chem. Rev.* **2000**, *100*, 421.
(24) Frisch, M. J.; Trucks, G. W.; Schlegel, H. B.; Scuseria, G. E.; Robb, M. A.; Cheeseman, J. R.; Zakrzewski, V. G.; Montgomery, J. A.; Stratmann, R. E.; Burant, J. C.; Dapprich, S.; Millam, J. M.; Daniels, A. D.; Kudin, K. N.; Strain, M. C.; Farkas, O.; Tomasi, J.; Barone, V.; Cossi, M.; Cammi, R.; Mennucci, B.; Pomelli, C.; Adamo, C.; Clifford, S.; Ochterski, J.; Petersson, G. A.; Ayala, P. Y.; Cui, Q.; Morokuma, K.; Malick, D. K.; Rabuck, A. D.; Raghavachari, K.; Foresman, J. B.; Cioslowski, J.; Ortiz, J. V.; Stefanov, B. B.; Liu, G.; Liashenko, A.; Piskorz, P.; Komaromi, I.; Gomperts, R.; Martin, R. L.; Fox, D. J.; Keith, T.; Al-Laham, M. A.; Peng, C. Y.; Nanayakkara, A.; Gonzalez, C.; Challacombe, M.; Gill, P. M. W.; Johnson, B. G.; Chen, W.; Wong, M. W.; Andres, J. L.; Head-Gordon, M.; Replogle, E. S.; Pople, J. A. *Gaussian 98*, revision A.9; Gaussian, Inc.: Pittsburgh, PA, 1998.
(25) Peng, C.; Ayala, P. Y.; Schlegel, H. B.; Frisch, M. J. *J. Comput. Chem.* **1996**, *17*, 49.
(26) Hay, P. J.; Wadt, W. R. *J. Chem. Phys.* **1985**, *82*, 270.
(27) Hay, P. J.; Wadt, W. R. *J. Chem. Phys.* **1985**, *82*, 299.
(28) Gonzalez, C.; Schlegel, H. B. *J. Phys. Chem.* **1990**, *94*, 5523.
(29) Reed, A. E.; Curtiss, L. A.; Weinhold, F. *Chem. Rev.* **1988**, *88*, 899.
(30) Siegbahn, P. E. M. *J. Comput. Chem.* **2001**, *14*, 1634.
(31) Chen, H.; Li, S.; Jiang, Y. *J. Phys. Chem. A* **2003**, 107, 4652.
(32) Warshel, A.; Levitt, M. *J. Mol. Biol.* **1976**, *103*, 227.
(33) Singh, U. C.; Kollman, P. A. *J. Comput. Chem.* **1986**, *7*, 718.
(34) Field, M. J.; Bash, P. A.; Karplus, M. *J. Comput. Chem.* **1990**, *11*, 700.
(35) Garcia-Viloca, M.; Gao, J.; Karplus, M.; Truhlar, D. G. *Science* **2004**, *303*, 186.
(36) Cui, Q.; Elstner, M.; Karplus, M. *J. Phys. Chem. B* **2002**, *106*, 2721.
(37) Hatcher, E.; Soudackov, A. V.; Hammes-Schiffer, S. *J. Am. Chem. Soc.* **2004**, *126*, 5763.
(38) Olsson, M. H. M.; Siegbahn, P. E. M.; Warshel, A. *J. Biol. Inorg. Chem.* **2004**, *9*, 96.
(39) Olsson, M. H. M.; Siegbahn, P. E. M.; Warshel, A. *J. Am. Chem. Soc.* **2004**, *126*, 2820.